An Evaluation of the Effects of Cloud Parameterization in the R42L9 GCM

WU Tongwen*[1,2] (吴统文), WANG Zaizhi[1] (王在志), LIU Yimin[1] (刘屹岷),
YU Rucong[1] (宇如聪), and WU Guoxiong[1] (吴国雄)

[1] *State Key Laboratory of Numerical Modeling for Atmospherics Sciences and Geophysical Fluid Dynamics, Institute of Atmospheric Physics, Chinese Academy of Sciences, Beijing* 100029

[2] *Laboratory for Climate Study, National Climate Center, Beijing* 100081

(Received 21 April 2003; revised 23 October 2003)

ABSTRACT

Cloud is one of the uncertainty factors influencing the performance of a general circulation model (GCM). Recently, the State Key Laboratory of Atmospheric Sciences and Geophysical Fluid Dynamics, Institute of Atmospheric Physics (LASG/IAP) has developed a new version of a GCM (R42L9). In this work, roles of cloud parameterization in the R42L9 are evaluated through a comparison between two 20-year simulations using different cloud schemes. One scheme is that the cloud in the model is diagnosed from relative humidity and vertical velocity, and the other one is that diagnostic cloud is replaced by retrieved cloud amount from the International Satellite Cloud Climatology Project (ISCCP), combined with the amounts of high-, middle-, and low-cloud and heights of the cloud base and top from the NCEP. The boreal winter and summer seasonal means, as well as the annual mean, of the simulated top-of-atmosphere shortwave radiative flux, surface energy fluxes, and precipitation are analyzed in comparison with the observational estimates and NCEP reanalysis data. The results show that the scheme of diagnostic cloud parameterization greatly contributes to model biases of radiative budget and precipitation. When our derived cloud fractions are used to replace the diagnostic cloud amount, the top-of-atmosphere and surface radiation fields are better estimated as well as the spatial pattern of precipitation. The simulations of the regional precipitation, especially over the equatorial Indian Ocean in winter and the Asia-western Pacific region in summer, are obviously improved.

Key words: cloud parameterization, effect of cloud on model performance, R42L9 model, climatological cloud scheme, diagnostic cloud scheme

1. Introduction

Clouds are global in nature and regularly cover about 50% of the earth according to earlier reports (e.g., Sellers, 1965) and about 60% in later observations (Berlyand et al., 1980; Warren et al., 1986, 1988; Mokhov and Schlesinger, 1994). A number of observational and modeling studies have shown the importance of clouds in climate and weather processes. Cloud amount is a key parameter to influence the radiation budget at the earth's surface and at the top of the atmosphere, and to influence precipitation. In most GCMs, cloud amount is very difficult to accurately diagnose or forecast. Moreover, its seasonal mean cannot be well simulated (Gates et al., 1999). In addition, the simulation of cloud optical properties is also a major problem (Manabe et al., 1991). Although results from the first phase of the Atmospheric Model Intercomparison Project (AMIP) demonstrated that current atmospheric models generally provide a realistic portrayal of the phase and amplitude of the seasonal march of the large-scale distribution of temperature, pressure, and circulation (Gates et al., 1999), the simulation of clouds and related processes account for most of the uncertainty in predicting climate change (IPCC, 2001).

During recent years, the State Key Laboratory of Atmospheric Sciences and Geophysical Fluid Dynamics, Institute of Atmospheric Physics (LASG/IAP) developed a new version of an atmospheric general circulation model AGCM, which is a spectral model truncated at R42 (approximately 2.8125°lon×1.66°lat) res-

*E-mail: twwu@cma.gov.cn

olution with nine vertical levels (hereafter R42L9). This model performs well in reproducing the observed basic patterns of atmospheric circulation and precipitation (Wu et al., 2003). Nevertheless, large regional biases still exist. It is important to analyze possible reasons leading to the weakness of climate simulation in the R42L9 model. Wu et al. (2003) noticed that diagnostic cloud amounts in the R42L9 model based on the cloud parameterization scheme developed by Slingo (1987) have large biases with respect to observations. The globally averaged annual mean of low cloud in the R42L9 model is about 22.9%, which is nearly 3% less than the International Satellite Cloud Climatology Project (ISCCP) observations (26%), and that of high cloud is about 23.6%, which is 10% more than the ISCCP cloud. In fact, similar biases also appear in other GCMs. The AMIP Modeling Groups (1996) estimated the zonally averaged cloud amount at each pressure level in 24 models participating in the AMIP and compared this with the ISCCP C2 data as well as with other observations. Their results showed that the global means of the model high cloud amount are about two to five times greater than the C2 satellite observations, while the globally averaged annual mean of the low cloud amount in most models is generally 10%–15% less than the C2 observations.

The influence of cloud uncertainty on model performance is our main concern. It is essential to evaluate the role of the present scheme of diagnostic cloud parameterization in the performance of the R42L9 model using the observed cloud data to replace the diagnostic cloud. This method would reduce errors of simulation resulting from cloud uncertainty. The data and method will be discussed in section 2. The effects of using two different cloud schemes on the R42L9 model mean climate will be evaluated in section 3. The main results are summarized in section 4.

2. Data and methods

In this work, 6-year (1985–90) monthly mean global 2.5°lon×2.5°lat. ISCCP total cloud amount, 6-year (1985–90) averaged monthly radiative fluxes at the top of the atmosphere from the Earth Radiation Budget Experiment (ERBE), 40-year (1958–97) averaged monthly radiative fluxes at the surface from the NCEP (U.S. National Centers for Environmental Prediction) reanalyses archive, and 22-year (1979–2000) averaged monthly precipitation from Xie and Arkin (1996) are used.

Clouds in the R42L9 model are allowed to form in any model layer. Nowadays, the total cloud amount and the height of the cloud top can be observed from both satellite and the ground. But the vertical structure inside a deep cloud column is very difficult to directly observe. Cloud amounts from the NCEP reanalyses data (Kalnay et al., 1996) serve as an important reference to estimate vertical distribution of cloud in the real atmosphere. We reconstructed the 20-year (1980–99) averaged climatology of NCEP cloud amount at pressure levels from the ground to 50 hPa at 50-hPa intervals utilizing the amounts of high, middle, and low clouds and pressures of the top and bottom of each cloud at four times every day. As shown in Fig. 1, the total cloud amounts still have some large biases compared with the ISCCP climatology not only in geographical distribution but also in magnitude, especially over the tropics of both hemispheres. As for the global annual mean, the total cloud amount (0.51) from NCEP reanalyses is less than that of the ISCCP climatology (0.62).

The vertical distribution of cloud in the real atmosphere can be approximately estimated if we modify the vertical profiles of the derived NCEP cloud data using the ISCCP total cloud amount. ISCCP satellite cloud amount data are of high quality. Mokhov and Schlesinger (1994) showed that there was good agreement between the ISCCP cloud amount and the ground-based data (Warren et al., 1986, 1988; Berlyand et al., 1980). We assume that there is a relationship between the observed total cloud amount $C_{\text{total, obs}}$ in the air column (i.e., ISCCP cloud amount in this study) and the observed cloud amount ($C_{k,\text{obs}}$ unknown variables) at given vertical layer k ($k = 1, 2, \ldots, K$) which is the number of vertical layers):

$$C_{\text{total, obs}} = 1 - (1 - C_{1,\text{obs}}) \times (1 - C_{2,\text{obs}}) \cdots (1 - C_{K,\text{obs}}) \,. \quad (1)$$

We then modify the vertical profile $C_{k,\text{obs}}$ using the derived NCEP cloud following the expression

$$C_{k,\text{obs}} = a_k \cdot C_{k,\text{NCEP}} \quad (k = 1, 2, \cdots, K) \,, \quad (2)$$

where a_k is a correction coefficient. Thus Eq. (1) can be rewritten as

$$C_{\text{total,obs}} = 1 - (1 - a_1 \cdot C_{1,\text{NCEP}})(1 - a_2 \cdot C_{2,\text{NCEP}}) \cdots (1 - a_K \cdot C_{K,\text{NCEP}}) \quad (3)$$

In Eq. (3), only $a_k (k = 1, 2, \ldots, K)$ is unknown. If we assume that a_k has little change with the height of cloud and is approximately taken as a constant independent of the layer, then Eq. (3) can be rewritten as

$$f(a) = 0 \quad (4)$$

where

$$f(a) = C_{\text{total, obs}} - [1 - (1 - a \cdot C_{1,\text{NCEP}}) \times (1 - a \cdot C_{2,\text{NCEP}}) \cdots (1 - a \cdot C_{K,\text{NCEP}})] \,. \quad (5)$$

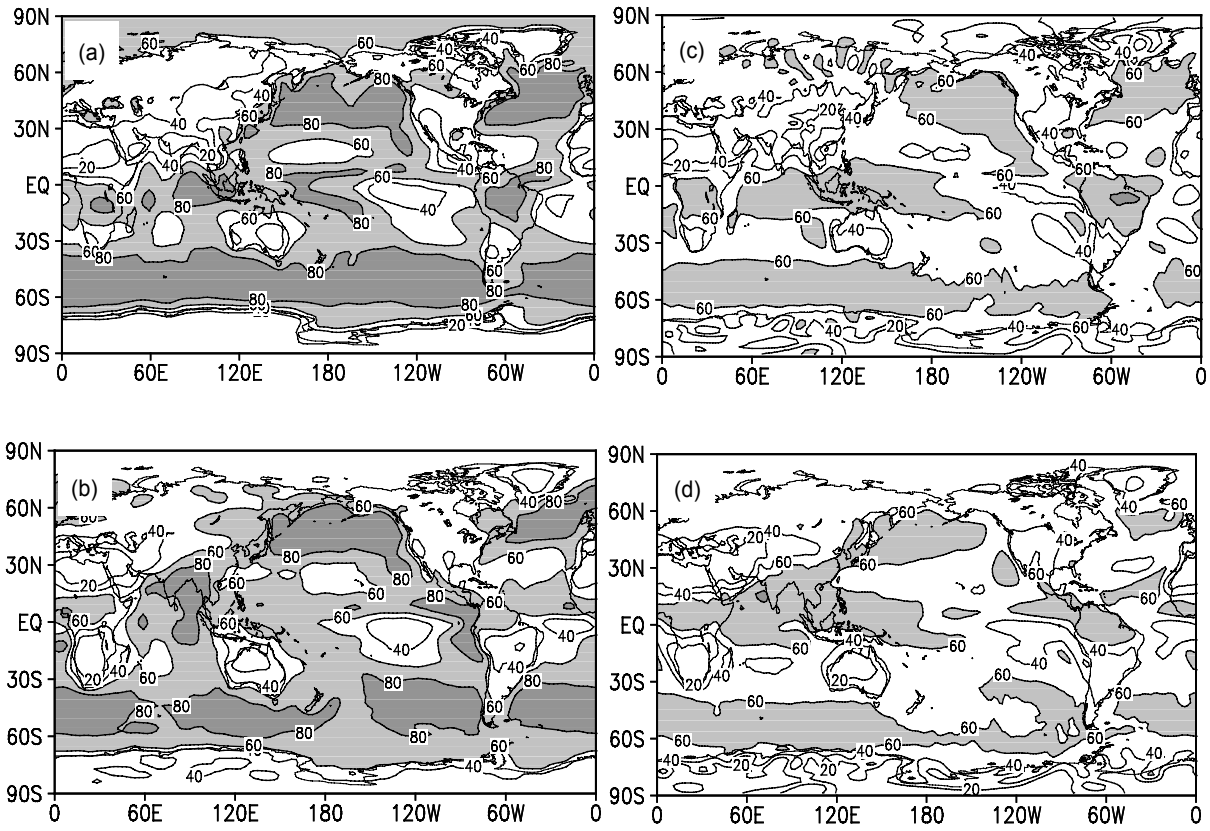

Fig. 1. January (a, c) and July (b, d) climatology of the total cloud amount (%) from ISCCP (left) and NCEP (right) data. The contour interval is 20% and the areas with values more than 60% are shaded.

In Eq. (4), there is only one unknown variable, namely a. It can be easily calculated using the following methods so that cloud amount $C_{k,\mathrm{obs}}$ at a given layer $k(k = 1, 2, \ldots, K)$ can be estimated following the expression (2). First, we know that the exact value of a in Eq. (4) must be larger than a minimum $a_{\min}$ that may be set to 0, and smaller than a maximum $a_{\max}$ that meets the condition $1 - a_{\max} \cdot C_{k,\mathrm{NCEP}} \geqslant 0$ for all $k(k = 1, 2, \ldots, K)$. From $a_{\min}$ and $a_{\max}$, we can easily pick out one for which the values $f(a)$ must be opposite to the value $f(a_{\mathrm{mid}})$ at their midpoint a_{mid}. So the range of the exact value of a in Eq. (4) is shortened and can be reset again. Using the same step above, the range of a is gradually made shorter and shorter and the exact value of a in Eq. (4) can be gradually approached.

We make a comparison of precipitation and radiative budget in the R42L9 model from a 20-year integration in which the diagnostic cloud scheme is replaced by our derived monthly mean cloud amount ($C_{k,\mathrm{obs}}$) at various pressures and climatological monthly mean sea surface temperatures and sea-ice fractional concentrations are used, with respect to another 20-year integration in which the diagnostic cloud scheme is adapted.

3. Validation of derived climate cloud in R42L9 model

3.1 *Classification of cloud types*

Clouds are conventionally classified into various types in terms of their position and appearance in the atmosphere. The microphysics of clouds in terms of particle size distribution and cloud thickness varies significantly with cloud type. Clouds from ground observation, as shown in Table 1, are usually classified into four types of low clouds, three types of middle clouds, and three types of high clouds, and those from ISCCP satellite observation are sorted into ten types of clouds. However, it is very difficult to accurately classify them in GCMs. Generally, only a few types of clouds can be considered according to the cloud height.

The detailed physical and numerical methods of the R42L9 model are described in previous papers (Wu et al., 1996; Zhang et al., 2000; Wu et al., 2003). Only five types of clouds are sorted in the R42L9 model (Table 1) on the basis of the cloud type and thickness presented by Liao (1992) and Stephens (1978). They

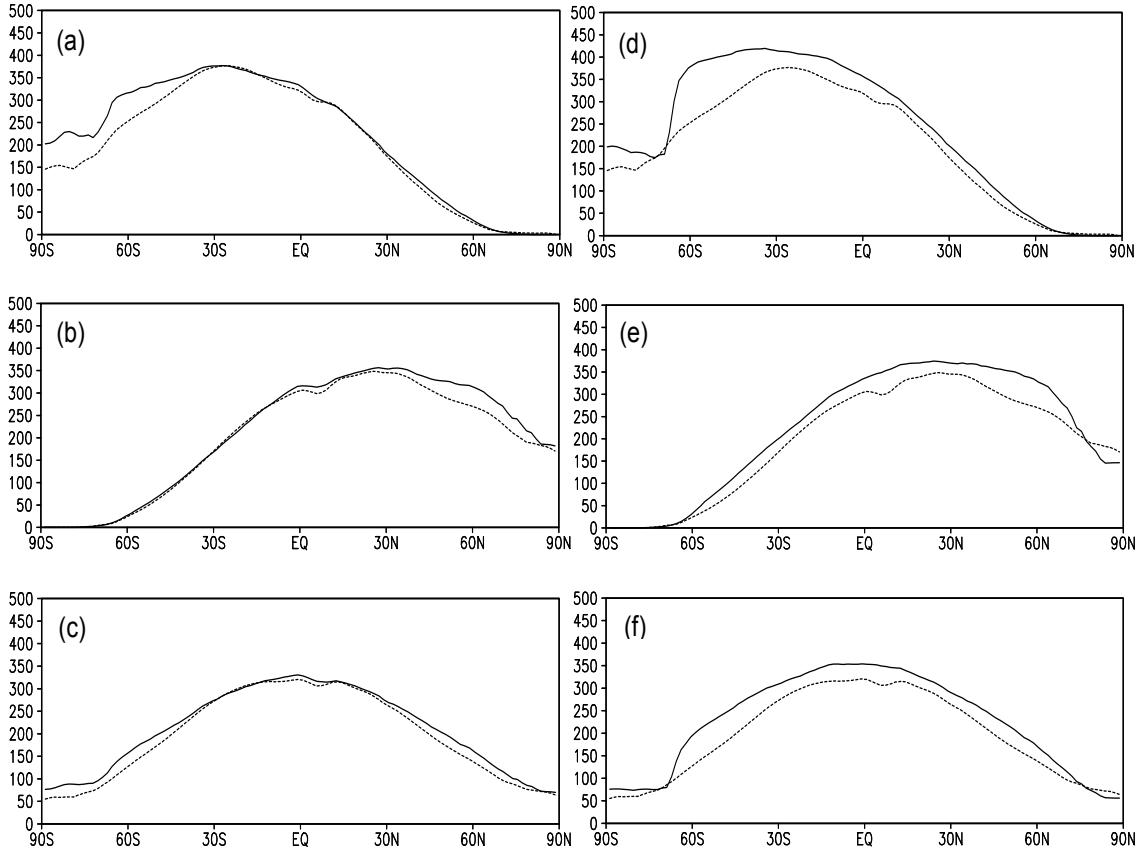

Fig. 2. Comparisons of zonal-mean for DJF (a, d), JJA (b, e), and the annual (c, f) absorbed shortwave radiation fluxes at the top of the atmosphere between the simulations by the R42L9 model (solid line) and the 6-year (1985–90) averaged ERBE climatology (dashed line). The solid lines in the left (a, b, and c) show the simulations forced by the climatological cloud, and those in the right (d, e, and f) by the diagnostic cloud scheme. Fluxes are in units of W m^{-2}.

match the present radiative parameterization scheme in the R42L9 model (Wang et al., 2000). As shown in Table 1, the clouds above 400 hPa, between 400 and 700 hPa, between 700 and 900 hPa, and below 900 hPa are regarded as cumulonimbus (Cb), altostratus (As), cumulus (Cu), and stratus (St), respectively. In addition, stratus is classified into two types, namely, stratus-I (St-I) over ocean and stratus-II (St-II) over land. As for all observed high clouds such as Cirrocumulus (Ci), Cirrus (Cc), and Cirrostratus (Cs), their optical properties are not considered in the present radiative parameterization scheme (Wang et al., 2000). High cloud in the R42L9 model is, at present, taken as cumulonimbus whose tops may reach the middle-cloud and high-cloud layers.

3.2 *Improvement of radiation budget*

Cloud has a large reflectivity to incident solar radiation. Variations of cloud amount and the height of the cloud top have large influences on the radiation budget, especially the shortwave radiation, at the top of the atmosphere. The zonal means of absorbed shortwave radiative fluxes at the top of the atmosphere from the R42L9 model and the ERBE data are shown in Fig. 2. When the diagnosed cloud scheme is used in the R42L9 model, as shown in Figs. 2d, 2e, and 2f, absorbed shortwave energy at the top of the atmosphere in boreal winter (December to February, DJF), summer (June to August, JJA), and the annual mean are obviously larger than the ERBE data. The largest biases in the R42L9 model appear at higher latitudes in summer hemispheres in both seasons. This overestimate of absorbed shortwave radiative fluxes implies that the upward shortwave flux in the R42L9 model is underestimated, which is partly attributed to a lower value of total cloud amount in the air column than the ISCCP observations (Wu et al., 2003). When the climatological cloud forcing is used to replace the diagnosed cloud, this deficiency is obviously reduced (Figs. 2a, 2b, and 2c). The absorbed fluxes agree with ERBE

Table 1. Ground-based, Satellite-based, and the R42L9 model's cloud classification schemes.

	Ground Based[a, b]	Satellite Based (ISCCP)[a, b]	R42L9 model
		Low Cloud	
Types[c]	St, Sc, Cu, Cb	Cu, Sc, St	St-I[e] (over ocean, Sfc-900 hPa) St-II[e] (over land, Sfc-900 hPa) Cu (900–700 hPa)
Vertical location	Sfc-2 km	Sfc-680 hPa	Sfc-700 hPa
		Middle Cloud	
Types	Ac, As, Ns	Ac, As, Ns	As
Vertical location	2–4 km (PL[d]) 2–7 km (ML[d]) 2–8 km (TL[d])	680–440 hPa	700–400 hPa
		High Cloud	
Types	Ci, Cc, Cs	Ci, Cc, Cs, DCC	Cb[f]
Vertical Location	3–8 km (PL[d]) 5–13 km (ML[d]) 6–18 km (TL[d])	440–50 hPa	Above 400-hPa

[a] Mokhov and Schlesinger (1994).

[b] Rossow and Schiffer (1991).

[c] Ac, Altocumulus; As, altostratus; Cb, Cumulonimbus; Cc, Cirrocumulus; Ci, Cirrus; Cs, Cirrostratus; Cu, Cumulus; DCC, deep convective cloud; Ns, Nimbostratus; Sc, stratocumulus; St, stratus.

[d] PL, polar latitudes; ML, middle latitudes; TL, tropical latitudes.

[e] St-I, stratus-I; St-II, stratus-II (Liao, 1992; Stephens, 1978).

[f] Cumulonimbus usually has its base in the low-cloud layer, but its top may reach the middle-cloud and high-cloud layers.

data well. In the latitudes of 30°S northward in DJF (Fig. 2a) and 30°N southward in JJA (Fig. 2b), the difference between the R42L9 simulation and the ERBE data is reduced to less than 10 W m^{-2}. The largest bias of about 50 W m^{-2} appears at higher latitudes of summer hemispheres both in DJF and in JJA. The bias partly results from the inaccurate description of cloud types in the R42L9 model (Table 1) because the high cloud in the real atmosphere usually appears in the form of ice cloud. In the present radiative parameterization scheme, the ice cloud is not yet treated.

Different cloud schemes in the R42L9 model also have a very important influence on the shortwave radiative fluxes at the ground surface. When the diagnostic cloud scheme is adopted, the model overestimates the net shortwave radiative energy absorbed by the ground surface. Remarkable biases of absorbed shortwave radiative fluxes at the surface with respect to the NCEP reanalysis data are found in the middle and lower latitudes of summer hemispheres in DJF (Fig. 3d) and JJA (Fig. 3e). The zonally averaged annual mean is about 100 W m^{-2} more than the NCEP data between 60°S and 30°S in boreal winter and approximately 60 W m^{-2} between 60°N and 30°N in boreal summer. The main contribution to these biases is that there is much more incident shortwave radiative fluxes at the surface than in the NCEP data (not shown). On the other hand, if using the climatological cloud forcing, the largest errors in the R42L9 model are reduced to about 30 W m^{-2} with respect to the NCEP reanalyses data (Figs. 3a, 3b, and 3c). The bias is almost within the scope of observational errors of shortwave surface flux. Kiehl and Trenberth (1997) noted that there is substantial uncertainty in observed shortwave surface flux around 25 W m^{-2} for the global annual mean.

Nearly a blackbody, cloud can emit downward longwave radiation. Low cloud amount and cloud-base height directly influence the variation of net longwave radiative fluxes at the surface. The zonally averaged surface net longwave radiative fluxes for DJF, JJA, as well as the annual mean from the R42L9 simulation and the NCEP reanalyses are shown in Fig. 4. When the cloud in the model is diagnosed, the amounts of the low cloud and the total cloud are underestimated (Wu et al., 2003) so that there is less amount of downward longwave flux emitted by the cloud back to the ground, resulting in more net upward longwave radiation from the surface emitted to the atmosphere (Fig. 4). The biases between the R42L9 simulation and the NCEP reanalyses are around 30 W m^{-2} for both seasons (Figs. 4d and 4e) and the annual mean (Fig. 4f).

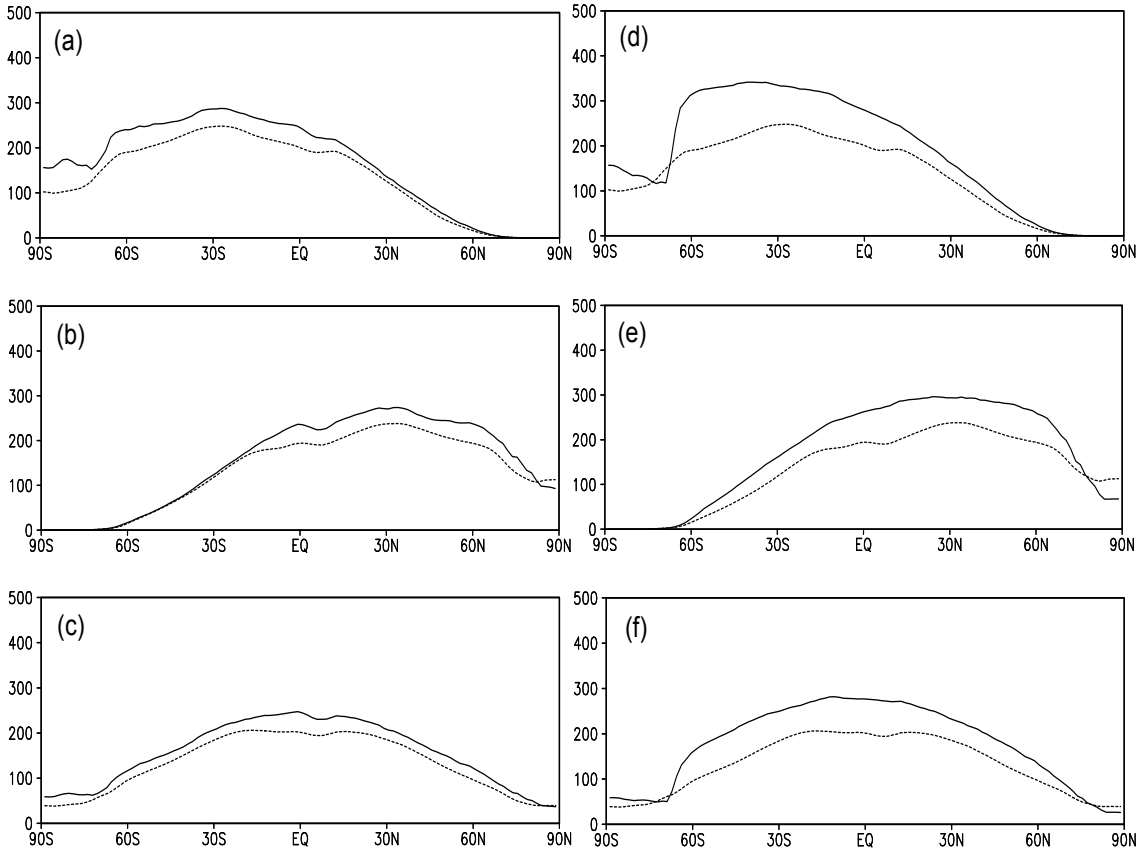

Fig. 3. The same as in Fig. 2, but for absorbed shortwave radiative fluxes at the surface from the R42L9 model (solid lines) and from the NCEP reanalysis (dashed lines).

This weakness of the R42L9 model is greatly improved when the diagnostic cloud is replaced by the climatological cloud. As shown in Figs. 4a–4c, the differences between the model simulation and the NCEP reanalyses are clearly reduced, especially in lower and middle latitudes of both hemispheres where there is about a 10 W m^{-2} bias.

From the above analyses, the large error of the radiative budget in the model is, to some extent, due to the incorrect description of cloud amount as well as its physical properties.

3.3 *Improvement of precipitation simulation*

Figure 5 illustrates the global distributions of DJF and JJA precipitation from the Xie and Arkin data and those from the R42L9 simulations. In boreal winter (DJF), large amounts of precipitation from Xie and Arkin's observations, as shown in Fig. 5c, are found in western South Africa, the South Indian Ocean, the Southeast Asia-western Pacific region, and the South American continent. In boreal summer (JJA), the regions with large amounts of precipitation are the Asian-Australian monsoon area and the northern tropics. When the diagnostic cloud scheme is used, the basic pattern of the observed precipitation is reproduced by the model. Nevertheless, there are some spatial errors in the simulation. For example, compared with the observations (Fig. 5f), there is too little precipitation in the southern tropical Indian Ocean, more precipitation in a meridionally narrowed belt of the southwestern Pacific in boreal winter (Fig. 5b), and less precipitation in the western part of the Indian Peninsula and in the eastern part of the equatorial Pacific in boreal summer (Fig. 5e)

When the climatological cloud amount is introduced into the R42L9 model, some weakness in the precipitation simulation is obviously improved. The spatial structure of the precipitation is much more similar to the observation than in the simulation using the diagnostic cloud scheme. In the boreal winter (DJF), the belt of large amounts of precipitation over the tropical South Indian Ocean from Xie and Arkin's data (Fig. 5c) is well reproduced (Fig. 5a). Its maximum is about 6 to 8 mm d^{-1}, which is close to the observation, and about 2–4 mm d^{-1} larger than that using the diagnostic cloud scheme. The precipitation

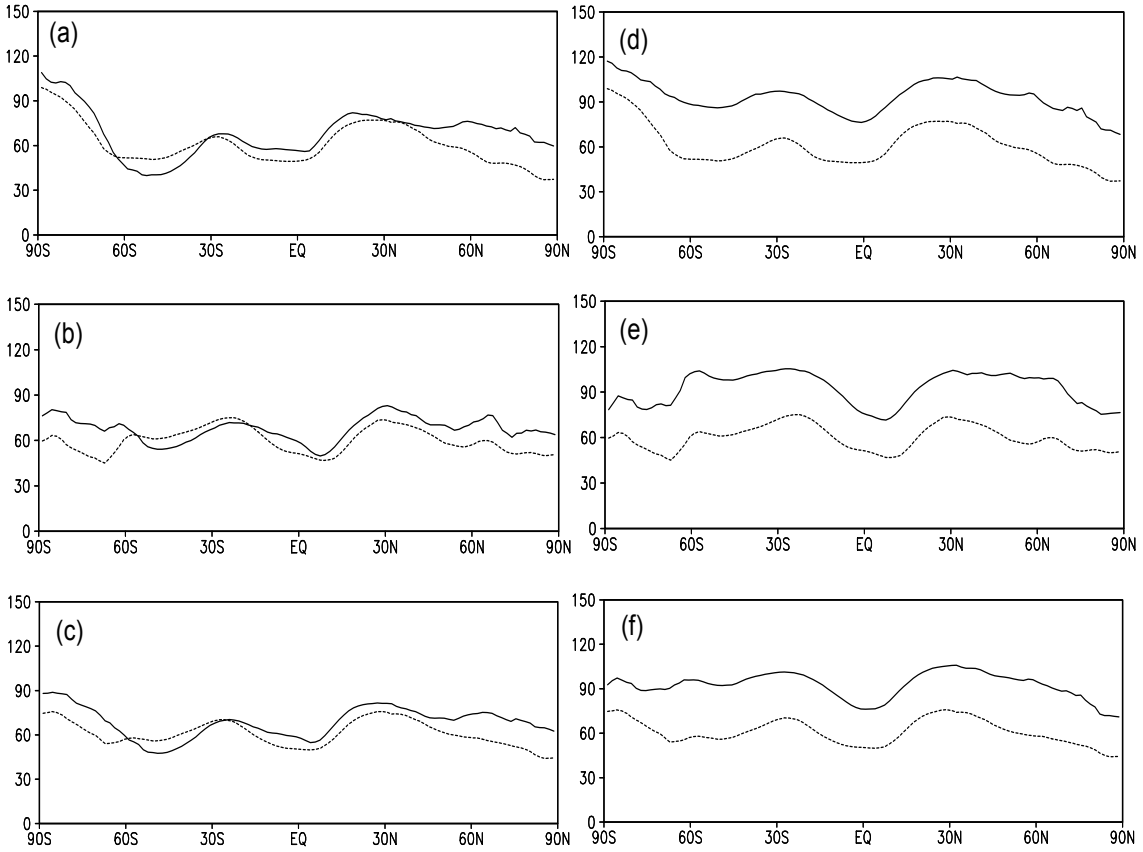

Fig. 4. The same as in Fig. 2, but for the net longwave radiation at the earth's surface.

over the western part of the equatorial Atlantic Ocean obviously increases and the rain belt spreads eastward to the central part of the equatorial Atlantic Ocean. In boreal summer, an obvious improvement in the precipitation simulation is found in the eastern part of the equatorial Pacific. Its maximum precipitation exceeds 8 mm d^{-1}, which is 4 mm d^{-1} larger than that using the diagnostic cloud scheme (Fig. 5e) and is closer to the observation (Fig. 5f). In addition, the R42L9 model reproduces well the spatial distribution of precipitation. An obvious maximum center of precipitation is found over the western part of the Indian Peninsula (Fig. 5d).

The improvement in the precipitation simulation can be seen in its zonal mean in boreal summer (Fig. 6). When the diagnosed cloud scheme is used in the R42L9 model, the maximum of simulated precipitation is about 2 mm d^{-1} less than that from Xie and Arkin's data (Fig. 6b). When the climatological scheme replaces the diagnosed cloud scheme, the precipitation is consistent with the observation (Fig. 6a).

Figure 7 shows the seasonal cycle of area-averaged precipitation (mm d^{-1}) over East Asia (22.5°–45°N, 105°–140°E), the Indian Monsoon Area (5°–30°N, 60°–105°E), and the whole of Asia (5°–45°N, 60°–150°E) from the R42L9 simulations and the Xie and Arkin's data. If we use the diagnostic cloud scheme, the seasonal variations of precipitation over the Indian monsoon region and the whole of Asia (Figs. 7d, 7e, and 7f) fail to be reproduced by the R42L9 model except for over East Asia. There is less precipitation than the observation from May to October averaged over the Indian monsoon region and the whole of Asia. The climatological cloud scheme improves the simulation. The annual cycles of regional mean precipitation over the Indian monsoon region and all of Asia (Figs. 7a, 7b, and 7c) agree with Xie and Arkin's data well. Especially during the prevailing period of the Asian summer monsoon from May to August, the intensity of area-averaged precipitation is consistent with the observation.

4. Summary

This paper describes a method to retrieve vertical profiles of cloud using ISCCP total cloud amount, combined with NCEP cloud data. In order to reduce the possible influence of inaccurate descriptions of cloud

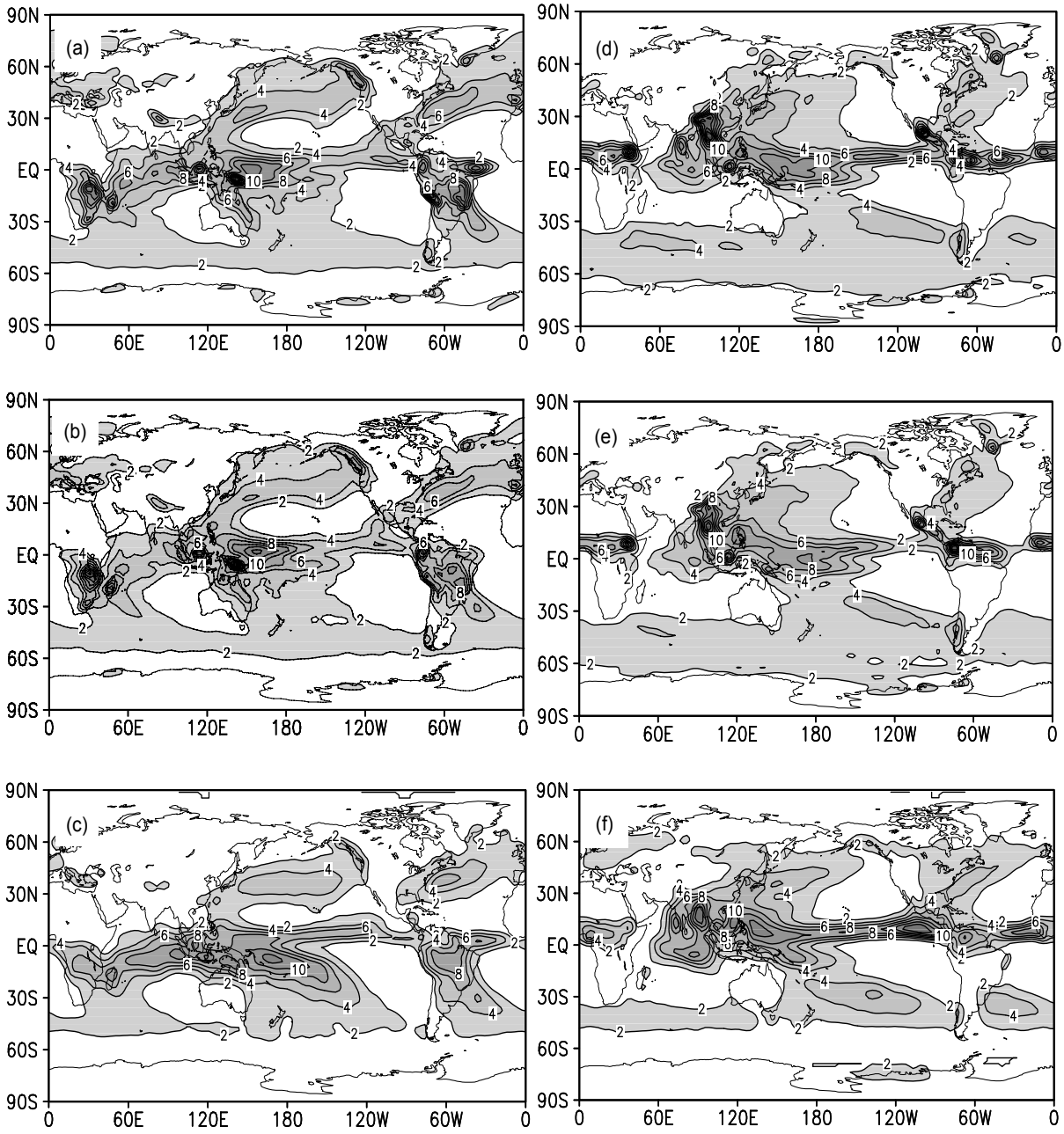

Fig. 5. Mean DJF and JJA precipitation (mm d^{-1}) of the R42L9 simulations forced by the climatological cloud (a, d) and by the diagnostic cloud (b, e) and Xie and Arkin's climatology (c, f). The areas where the precipitation rate is more than 2 mm d^{-1} are shaded. The contour interval is 2 mm d^{-1}.

in the R42L9 model on climatic simulation errors, the retrieved cloud amount in the model layers are used to replace the diagnostic cloud and then evaluate the roles of cloud in the model performance. A detailed comparison of the simulated shortwave radiative flux at the top of the atmosphere, surface energy fluxes, and precipitation with respect to those using the diagnostic cloud is presented. The potential advantage of using the climatological cloud scheme in the R42L9 model is not only a better simulation of the surface radiation fields but also a better reproduction of the observed spatial distribution of precipitation. In particular, the upward shortwave flux at the top of the atmosphere reflected back into space by the earth-atmosphere system and the downward longwave flux at the surface emitted by cloud and the atmosphere are obviously improved. Regional precipitation over the equatorial Indian Ocean in boreal winter and that

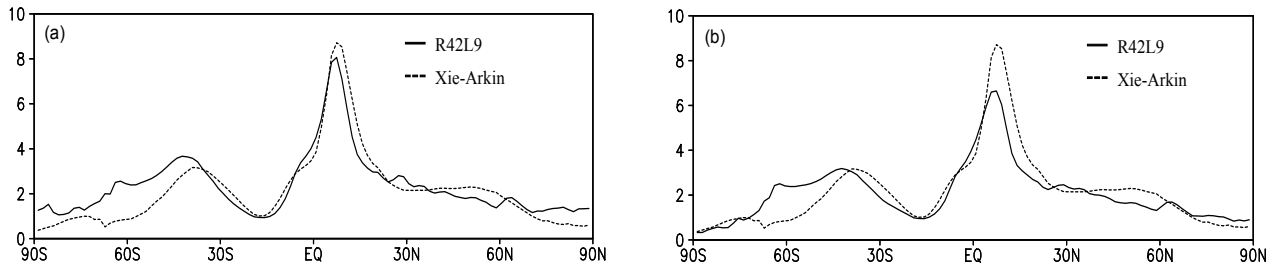

Fig. 6. Comparisons between the zonal-mean JJA precipitations (mm d^{-1}) from the R42L9 simulations and Xie and Arkin's climatology. The solid lines in (a) and (b) are the simulations forced by the climatological cloud and the diagnostic cloud schemes, respectively.

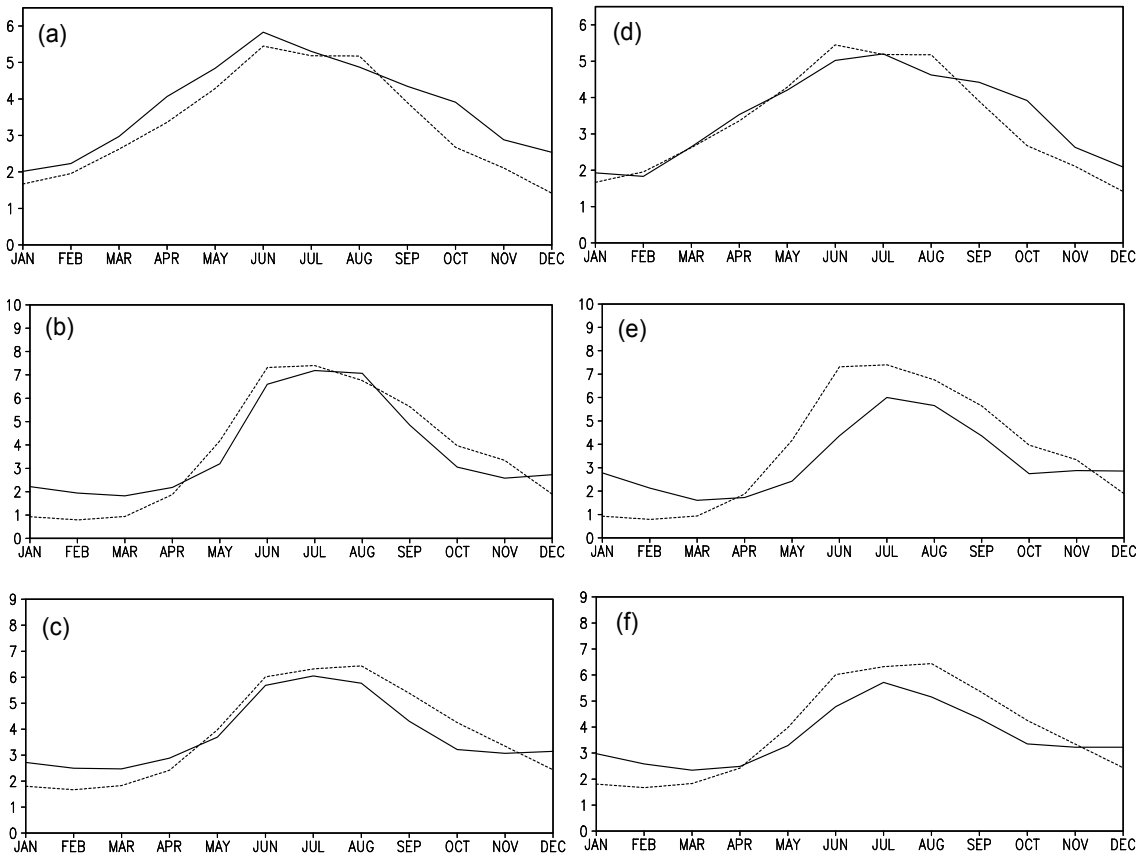

Fig. 7. Seasonal cycle of precipitation (mm d^{-1}) over East Asia (22.5°–45°N, 105°–140°E) (a, d), the Indian Monsoon area (5°–30°N, 60°–105°E) (b, e), and the whole of Asia (5°–45°N, 60°–150°E) (c, f) from the R42L9 simulations and the 22-yr (1979–2000) Xie and Arkin's climatology. The solid lines in the left panel show the simulations forced by the climatological cloud and those in the right panel by the diagnostic cloud scheme.

over the eastern equatorial Pacific and the western Indian Peninsula in boreal summer are well reproduced. The seasonal variations of area-averaged precipitation over the whole of Asia, East Asia, and the Indian monsoon areas are more reasonable. The present scheme of diagnostic cloud parameterization in the R42L9 model is responsible for the large difference between simulation and observation.

Acknowledgments. We would like to thank NCAR for providing the Xie and Arkin rainfall data, the ERBE data archives, and the NCEP/NCAR reanalysis data. We also thank Prof. Shi Guangyu and Prof. Weng Hengyi for their helpful comments. This work was jointly supported by the Chinese Academy Project ZKCX2-SW-210 and the Na-

tional Natural Sciences Foundation of China under Grant Nos. 40135020, 4023105, 40233031, and 40005008.

REFERENCES

AMIP Modeling Groups, 1996: Evaluation of the Vertical Structure of Zonally Averaged Cloud amount and Its Variability in the Atmospheric Model Intercomparison Project. *J. Climate,* **9**, 3419–3431.

Berlyand, T. G., L. A. Strokina, and L. E. Greshnikova, 1980: Zonal cloud distribution on the Earth. *Meteor. Hydrol.*, **3**, 9–15.

Gates, W. L., and coauthors, 1999: An Overview of the Results of the Atmospheric Model Intercomparison Project (AMIP I). *Bull. Amer. Meteor. Soc.,* **80**, 29–55.

IPCC, 2001: *Climate Change 2001, The Scientific Basis.* Contribution of Working Group I to the Third Assessment Report of the Intergovernmental Panel on Climate Change, J. T. Houghton, Y. Ding, D. J. Griggs, M. Noguer, P. J. Van Der Linden, X. Dai, K. Maskell, and C. A. Johnson, Eds., Cambridge University Press, Cambridge, United Kingdom, and New York, NY, USA, 892pp.

Kalnay, E., and coauthors, 1996: The NCEP/NCAR 40-year reanalysis project. *Bull. Amer. Meteor. Soc.*, **77**, 437–471.

Kiehl, J. T., and K. E. Trenberth, 1997: Earth's annual global mean energy budget. *Bull. Amer. Meteror. Soc.*, **78**, 197–208.

Liao, K. N., 1992: *Radiation and Cloud Processes in the Atmosphere.* Oxford University Press, New York, 487pp.

Manabe, R., J. Stouffer, M. J. Spelman, and K. Bryan, 1991: Transient responses of a coupled ocean-atmosphere model to gradual changes of atmospheric CO_2. Part 1: Annual mean response. *J. Climate*, **4**, 785–818.

Mokhov, I. I., and M. E.Schlesinger, 1994: Analysis of global cloud amount. *J. Geophys. Res.*, **99**, 17045–17065.

Rossow, W. B., and R. A. Schiffer, 1991: ISCCP cloud data products. *Bull. Amer. Meteor. Soc.*, **72**, 2–20.

Sellers, W. D., 1965: *Physical Climatology.* University of Chicago Press, Chicago, 272pp.

Slingo, J. M., 1987: The development and verification of a cloud prediction scheme for the ECMWF model. *Quart. J. R. Meteor. Soc.*, **113**, 899–927.

Stephens, G. L., 1978: Radiation profiles in extended water clouds: Theory. *J. Atmos. Sci.*, **35**, 2111–2122.

Wang Biao, Liu Hui, and Shi Guangyu, 2000: Chapter 3 Radiation and cloud scheme. *IAP Global Ocean-Atmosphere-Land System Model*, Zhang Xuehong, Shi Guangyu, Liu Hui, and Yu Yongqiang, Eds., Science Press, Beijing, New York, 28–49.

Warren, S. G., C. J. Hahn, J. London, R. M. Chervin, and R. L. Jenne, 1986: Global distribution of total cloud amount and cloud type amounts over land. NCAR Tech. Note TN-273+STR, Natl. Cent. for Atmos. Res., Boulder, Colo. 173pp.

Warren, S. G., C. J. Hahn, J. London, R. M. Chervin, and R. L. Jenne, 1988: Global distribution of total cloud amount and cloud type amounts over the ocean. NCAR Tech. Note TN-317+STR, Natl. Cent. for Atmos. Res., Boulder, Colo. 154pp.

Wu, Guoxiong, Liu Hui, Zhao Yucheng, and Li Weiping, 1996: A nine-layer atmospheric general circulation model and its performance. *Adv. Atmos. Sci.*, **13**, 1–18.

Wu, Tongwen, Liu Ping, Wang Zaizhi, Liu Yimin, Yu Rucong, and Wu Guoxiong, 2003: The performance of atmospheric component model R42L9 of GOLAS/LASG. *Adv. Atmos. Sci.*, **20**, 726–742.

Xie , P., and P. A. Arkin, 1996: Analyses of global monthly precipitation using gauge observations, satellite estimates, and numerical model predictions. *J. Climate*, **9**, 840–858.

Zhang Xuehong, Shi Guangyu, Liu Hui, and Yu Yongqiang, 2000: *IAP Global Ocean-Atmosphere-Land System Model.* Science Press, Beijing, 252pp.